Visual observations of streaking corrosion of aluminum alloys AA7075 and AA8006 in chloride solution

Ruo-Shuang Huang,[a,b] Chang-Jian Lin,[b,*] and Hugh S. Isaacs [a,**,z]

[a]*Brookhaven National Laboratory, Upton, NY 11973, USA*

[b]*State Key Laboratory for Physical Chemistry of Solid Surfaces, Department of Chemistry, Xiamen University, Xiamen 361005, China*

* Electrochemical Society Active Member.

** Electrochemical Society Fellow.

z E-mail: isaacs@bnl.gov

The surface behavior of aluminum alloys in chloride solutions has attracted considerable attentions because of its importance in corrosion.[1-10] Many alloys are susceptible to filiform corrosion which takes place under coatings.[1-6,11] Susceptibility has been correlated with specific electrochemical characteristics of a thin surface layer formed by thermomechanical treatment during manufacture.[1-6] Zn containing aluminum alloys also show a surface susceptibility in chloride solutions but for these alloys the surface sensitivity results from machining[7] and abrasion.[8-10] The surface attack takes place preferentially along grooves[8,10] producing streaks. Another similarity with all these alloys when sensitive to these types of corrosion is apparent in their polarization curves. Both sets of the alloys show a current peak associated with transient dissolution of the thin surface layer appearing only during the first potential scan from around the open circuit potential to where pitting corrosion takes place.[4-6,9,10]

The present work employs a new imaging technique[10,12] to study changes taking place on surfaces and describes measurements that show a further similarity. AA8006, an alloy susceptible to filiform corrosion, has been found to display streaking corrosion similar to that seen with AA7075 and other Zn containing alloys.[8-10]

Experimental

Samples were cut from a 5 mm thick plate of AA7075-T6 with a weight percent

composition of 5.5 Zn, 2.5 Mg, 1.5 Cu, 0.2 Cr and a fully annealed 1 mm thick sheet of AA8006-O with a nominal composition in weight percent of 1.5 Fe, 0.4 Mn, 0.2 Si, 0.02 Mg. The alloys were tested after wet abrasion on SiC paper, and following etching, and heating the abraded surface in air. AA8006 was also tested in the as-received condition. Etching was in 1.0 M NaOH at 60^{o}C for 1.5 min followed by immersion in 70 % HNO_3 for 0.5 min.

Transparent adhesive tape (3M Co. Type 5) with a 6x6 or 5 x 5 mm^2 window was applied to sample areas >30 x 30 mm^2 to restrict the exposed area during testing. The sample formed the base of a closed test cell with walls of a square 25 x 25 mm^2 plastic cylinder and a transparent lid through which the exposed surface was optically monitored. A saturated Ag/AgCl reference electrode (-50mV vs. a saturated calomel electrode) and a Pt wire counter electrode were inserted through holes in the lid. About 12 cm^3 of solution completely filled the cell. Open circuit potential, cyclic polarization at 0.2 mV s^{-1} and constant current measurements, starting about 50mV below the open circuit potential, were made. The solution used was air saturated 0.5 M NaCl. In some experiments, to observe pH changes, 5% by volume of a wide-range pH indicator (Fisher, Universal Indicator) was added to the NaCl solution.

The surfaces tested were under continuous optical surveillance using a difference viewer imaging technique (DVIT) (Applicable Electronics Inc.) which displayed both a real-time image and a processed difference-image. The difference image was

obtained by digital subtraction of an earlier image from the real time image. The difference was further processed by multiplying the result by an amplification factor and adding a grey level to the entire image. The resulting processed image showed only changes that took place during the period between recording the earlier background image and the real time image.[12] The processed difference-images are unencumbered by visible "noise" created by static details in a real time image and only identified where changes have taken place on the surface or in solution. In addition, the electrochemical current and potential parameters are recorded in conjunction with each real time image.

Results

In combination, the DVIT and the electrochemical data yielded specific information of *in situ* surface changes, which were very difficult to correlate using common *in situ* imaging techniques. An *in situ* image of the surface of abraded AA7075 exposure to 0.5 M NaCl for 10 min is shown in Fig. 1a. The abrasion marks on the surface are 45^{o} and the edges of the transparent tape can be seen. The discernable changes during the exposure were difficult to define both in real time and on reviewing recorded images. However, the difference image in Fig. 1b derived from the 10 min image in Fig. 1a and earlier image, at 7 min, shows that many streaks, seen as thin lines that had grown in the 3 min period predominantly along a single abrasion groove. Fig. 1c is a magnified area of Fig. 1b. The arrow A points to the site where a

streak initiated and grew in both directions. Streaks grew at rates which varied from site to site. Some streaks continued to grow, others terminated, and new sites initiated. Maximum rates were about 6 μm s^{-1}.

Potentiodynamic current measurements in Fig. 2 for AA7075 produced no visible attack below the open circuit potential, -720 mV, and streaking began at and above this potential. Unlike the streaks at open circuit which ran within a single groove, the attack was predominantly in bands incorporating many adjacent abrasion grooves. The streaking showed a preference for propagating from the edge of the tape into the exposed area with some penetrations under the tape. Fig. 1d, a difference image, shows this surface attack during a 3 min period when the current density in Fig. 2 reached 0.62 mA cm^{-2}. The thickness of the bands, the tendency to propagate underneath the tape, and presence of bubbles all increased with potential. About 50 % of the exposed area was streaked when the current reached a maximum and covered the entire surface at -680mV when a current minimum was recorded. The charge on integrating the current over the period of the peak was 151 mC cm^{-2}. Once an area was etched by the streaking, streaking did not take place again. No indication of a peak was seen on decreasing the potential after reversal of the scan direction at a potential above the peak.

Experiments with additions of a pH indicator to simple solutions were carried out similar to those in viscous electrolytes with sucrose, and in gels, all containing

chlorides.[8] In these environments a low pH was observed around and behind the growing tips of streaks which faded when streaking stopped. In viscous electrolytes a number of new streaks were seen to initiate when a low pH convection plum produced by a growing streak touched down on another area of the Al surface. In simple aqueous electrolytes the very low pH regions at the growing streaks were rapidly diluted by convection establishing large areas of pH lower than the bulk pH of ~6 which were also more prone to streaking.

Streaking of AA7075 has been associated with the presence of a surface layer[10] and ion milling or etching the surface of abraded Al-Zn alloy in NaOH followed by HNO_3 removed the formation of streaking at open circuit and led only to pitting during potentiodynamic polarization.

As received AA8006 showed somewhat similar characteristics to the abraded AA7075 but the AA8006 was more prone to pitting. Streaking was observed from DVIT images during open circuit, as shown in Fig. 3a. Several horizontal fine darkened streaks grew along the rolling direction. There were far fewer active streaking sites compared with abraded AA7075 but the propagation rates were similar. Streaking was stopped below the open circuit potential at the start of potentiodynamic scans. It started again when the prior open circuit potential was reached. Fig. 3b shows a difference image derived from -766 mV (0.5 mA cm^{-2}) and -802 mV surfaces. At higher currents the initiation of streaking on adjacent grooves was greater than that

seen with the Zn alloy, leading to more spreading perpendicular to the rolling direction. The polarization curve in Fig. 2 showed a shoulder as streaking covered the surface on first increasing the potential followed by a dramatic appearance of pitting as the current continued to increase.

In other experiments after abrasion of AA8006, no streaking could be seen at open circuit or during potentiodynamic polarization. Only pitting took place above a significantly higher potential e.g. -710 mV in 1M NaCl. Abrasion and heating at 600^{o}C for 2 h gave streaking but only at low current densities and at a more negative potential of -800 mV. At higher currents and potentials the behavior was different. The streaking sites began to pit and any new site behaved as an active pit evolving bubbles.

With additions of a pH indicator AA8006 produced results similar to those seen with AA7075 where acidity developed around the head of active streaking lines as they moved along the rolling direction.

Discussion

Al-Zn alloys[7,9,10] and those showing filiform corrosion have an active surface layer[1-3,14,15] that leads to a polarization curves with a current peak that has been referred to as second breakdown potential[9,13], at lower potentials than that for pitting.

Maitra and English considered the differences in potential with abraded AA 7075 to result from grain boundary enrichment and differences between grain boundary regions and the grain interiors due to precipitation of Mg, Zn, and Cu.[13] Meng and Frankel attributed the electrochemical susceptibility to attack of fine hardening particles containing Cu in the surface layer and the accompanying dissolution of the surrounding Al matrix.[9] Afseth et al.[1] have reviewed enhanced surface shear deformation of Al during rolling where the more brittle micrograined surface layers break-up and becomes “smeared over by the softer, underlying metal, or they fold over and reweld to the surface” and redistribution of very fine particles of intermetallics and incorporated oxide phases that inhibited recrystallizaton by Zenner pinning.[1] Also discussed are associated effects on the solubility and intermetallic formation.[1] More recent models attribute the sensitivity of the layer to the presence of Pb that diffuses to the surface along the high density of grain boundaries during heat treatment. [4-6,14,15]

DVIT results Figs. 1 and 3 show streaking corrosion of AA7075 and A8005. The possible presence of streaking corrosion with AA8006 was investigated because of the distinct similarity in the polarization curves for alloys that are susceptible to filiform corrosion[4-6] and for polarization curves of Al-Zn alloys.[9,10] The streaking of both alloys correlated directly with the increased currents in the polarization curves in Fig. 2 at potential below where high currents due to localized pitting dominated. The distinct peak for AA7075 in Fig. 2 resulted from a charge of 151 mC cm^{-2} which

corresponds to oxidation of a 50 nm layer of Al. This may be an underestimate of the Al layer thickness because bubbles of a gas, probably hydrogen, were apparent. If the hydrogen was associated with the attack of the surface layer then the observed anodic current underestimates the charge by the amount extracted by hydrogen formation. If the hydrogen formation follows the same route as in pitting the error would be of the order of 15%.[16] Meng and Frankel derived a thickness of about 75 nm from current transients at fixed potentials.[9] Similar measurements were reported by Huang et al. on removal of surface layers chemically or by ion milling.[10]

The polarization behavior on the first cycle for AA8006 in Fig. 2 shows a shoulder on polarization around –740 mV. Again the presence of the increased current correlated directly with streaking using DVIT and the associated charge may be roughly estimated within the range observed with AA7075. A closer estimate is dependent on judging the background current associated with pitting. Certainly bubbles were more numerous during streaking, than with AA7075. Keuong et al.[5] potentiostatically polarized as received AA8006 at a potential close to the current minimum above an observed current peak and found a charge of 187 mC cm^{-2} or about 62 nm a thickness of the same magnitude as that found for the susceptible layer on AA7075. Nisancioglu and co-workers report the presence of a limited susceptible surface region based on potentiodynamic, open circuit potential transients, and current transients. Their studies included AA8006, and the AA1000, and 3000 alloy series.[1-6,14,15] The work showed that abrasion removed the surface susceptibility

produced on heating or during thermomechanical manufacture. It distinctly contrasts with the surface susceptibility of Zn containing Al alloys that is brought on by abrasion. Further measurements are required to determine the range of alloys and their pre-treatments that will produce streaking corrosion.

The streaking corrosion observed with both AA7075 and AA8006 takes place by a similar process as judging from pH changes using indicators. Low pH results from hydrolysis of dissolved Al ions around the growing streak. A mechanism for streak propagation following initiation can be based on the high aluminum chloride concentration and associated low critical pH ahead of a growing streak initiating further breakdown. The very rapid streaking rate of 6 μm s^{-1} corresponds to a current density of 18 A cm^{-2} and is within the order of magnitude found for initial pit growth.[17] In contrast to pits that grow in volume under the passive layer, the low pH developed around the growing tip of a streak leads to further breakdown of passivity ahead of the streak.

The groove geometry of the growing streak influences the mode of growth. The grooves help to confine the low pH necessary for breakdown. This critical pH is reached within the groove but at its edges diffusion into the bulk solution is comparatively unrestricted and rapid dilution raises the pH above the critical value preventing corrosion starting in adjacent grooves. However, during polarization the rate of dissolution increases, increasing concentrations, and enables spillover of the

critical low pH to adjacent grooves. The streaks then become broader as seen in Figs. 1d and 3b.

The relative breakdown potentials for streaking and pitting may be important in the pitting behavior of many Al alloys. The potentiodynamic polarization curve for AA7075 in Fig. 2 displays a clear separation between streaking and pitting, whereas for AA8006 the presence of streaking is less clear and leads only to a shoulder. A schematic showing the relative positioning of the two phenomena in Fig. 4 maintains a fixed breakdown behavior for streaking and a variable pitting behavior. It is assumed that their currents can simply be added together. In practice it is found that not only will both changes with surface preparation, heat treatments, chloride concentration, pH of the test solution, and potential sweep rate[4,6,13] but the streaking, if within the range of pit growth can initiate pitting sites. This assisted initiation was observed with abraded AA8006 heat treated at 600^{o}C which showed little tendency to streak and inhibited streaking at higher potentials. These observations suggest that the susceptible layer can act as a pit initiator. Characteristics of pit initiation sites are generally difficult to identify and future studies of the causes of the surface susceptible layer may also lead to a deeper understanding of pit initiation.

Conclusions

Streaking corrosion along grooves has been observed in chloride solutions on a Zn containing Al and an alloy susceptible to filiform corrosion using an *in situ* image difference technique. A thin susceptible layer of the order of 50 nm in thickness is present which is removed during streaking. In the former alloy the layer is formed by abrasion while in the latter, by thermomechanical treatments. The propagation of the streaks is dependent on acidity at the tip of the growing streak confined by the grooves. Depending on the relative potentials at which streaking and pitting corrosion propagate, the presence of the susceptible layer can initiate pitting if it propagates more rapidly than streaking corrosion.

Acknowledgements

This work was conducted at Brookhaven National Laboratory under the auspices of the U.S. Department of Energy, Division of Materials Sciences, Office of Science, under contract no. DE-AC02-98CH10886. The authors wish to thank Kenneth Sutter for experimental assistance, Applicable Electronics Inc. for the use of the software and equipment used to acquire and manipulate the digital images, and A. Afseth, Novelis Technology AG, for supplying the AA8006.

References

1. A. Afseth, J. H. Nordlien, G. M. Scamans, K. Nisancioglu, *Corros. Sci.*, **43**, 2093 (2001).
2. A. Afseth, J. H. Nordlien, G. M. Scamans, K. Nisancioglu, *Corros. Sci.*, **43**, 2359 (2001).
3. A. Afseth, J. H. Nordlien, G. M. Scamans, K. Nisancioglu, *Corros. Sci.*, **44**, 145 (2002).
4. Y. W. Keuong, J. H. Nordlien, K. Nisancioglu, *J. Electrochem. Soc.*, **148**, B497 (2001).
5. Y. W. Keuong, J. H. Nordlien, K. Nisancioglu, *J. Electrochem. Soc.*, **150**, B547 (2003).
6. J. T. B. Gundrsen, A. Aytec, S. Ono, H. H. Nordhien, K. Nisancioglu, *Corros. Sci.*, 46, 265 (2004).
7. P. J. E. Forsyth, *Mat. Sci. Technol.*, **14,** 151 (1998).
8. H. S. Isaacs, G. Adzic, C. S. Jeffcoate, *Corrosion*, **56**, 971 (2000).
9. Q. J. Meng, G. S. Frankel, *J. Electrochem. Soc.*, **151**, B271 (2004).
10. R. S. Huang, C. J. Lin, H. S. Isaacs, in *Pits and Pores II: Formation, Properties and Significance for Advanced Materials*, P. Schmuki, Editor, The Electrochemical Society Proceedings Series, Pennington, NJ (2004).
11. G. M. Hoch, A Review of Filiform Corrosion, in *Localized Corrosion*, R. F. Brown, J. Kruger, R. F. Staehle, Editors, NACE, Houston (1974).

12. H. S. Isaacs, A. Haughton, A. M. Shipley, H. Popenoe, E. Karplus, J. B. Lumsden, in *Corrosion and Protection of Light Metal Alloys*, R. G. Buchheit, R. G. Kelly, N. A. Missert, B. A. Shaw, Editors, PV 2003-23, The Electrochemical Society Proceedings Series, Pennington, NJ (2003).
13. S. Maitra, G. C. English, *Metall. Trans. A.*, **12**, 535 (1981).
14. H. Leth-Olson, K. Nisancioglu, *Corros. Sci.*, **40**, 1179 (1998).
15. H. Leth-Olson, A. Afseth, K. Nisancioglu, *Corros. Sci.*, **40**, 1195 (1998).
16. E. Akiyama, G. S. Frankel, *J. Electrochem. Soc.*, **146**, 4095 (1999).
17. G. S. Frankel, R. C. Newman, C. V. Jahnes, M. A. Russak, *J. Electrochem. Soc.*, **140**, 2192 (1993).

Figure Captions.

Fig. 1. Images of AA7075 in 0.5 M NaCl. (a) A real image after open circuit exposure for 10 min. (b) A difference image derived from subtraction of an image at 7 min from an image at 10 min, amplifying the difference and adding a grey background. (c) Magnification of the area shown in (b). (d) A difference image derived from an image at a current density of 0.62 mA cm^{-2} and a 3 min earlier image recorded during the polarization scan shown in Fig. 2.

Fig. 2. Polarization curves for abraded AA7075 and as received AA8006 in 0.5 M NaCl at a scan rate of 0.2 mV s^{-1}.

Fig. 3. Images of as received AA8006 in 0.5 M NaCl. (a) A difference image obtained after subtracting and processing an image taken at 10 min from an image at 13 min. (b) A difference image derived from an image at a current density of 0.5 mA/cm2 and a 3 min earlier image during the polarization scan shown in Fig. 2.

Fig. 4. Schematic polarization curves showing the effects of changing the relative positions of the streaking and pitting susceptibility.

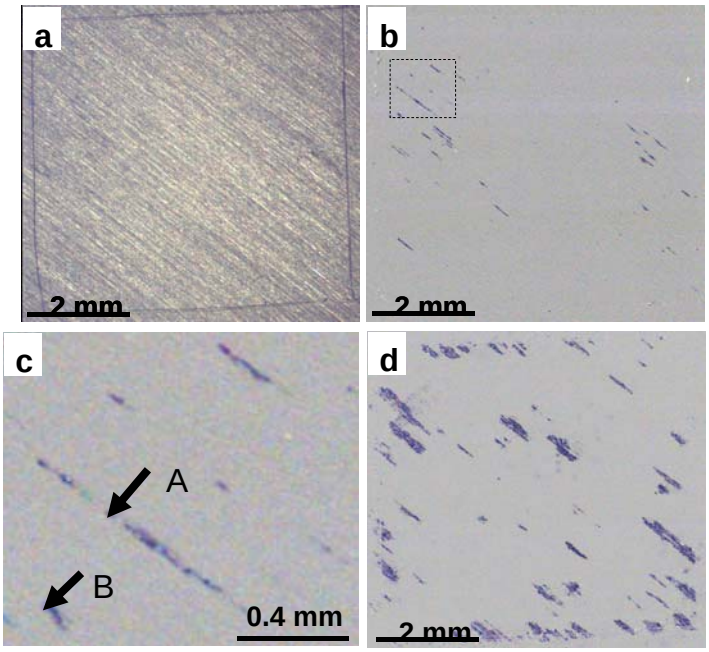

Figure 1. Images of AA7075 in 0.5 M NaCl (a) A real image after open circuit exposure for 10 min.

(b) A difference image derived from subtraction of an image at 7 min from an image at 10 min, amplifying the difference and adding a grey background.

(c) Magnification of the area shown in (b).

(d) A difference image derived from an image at a current density of 0.62 mA/cm2 and a 3

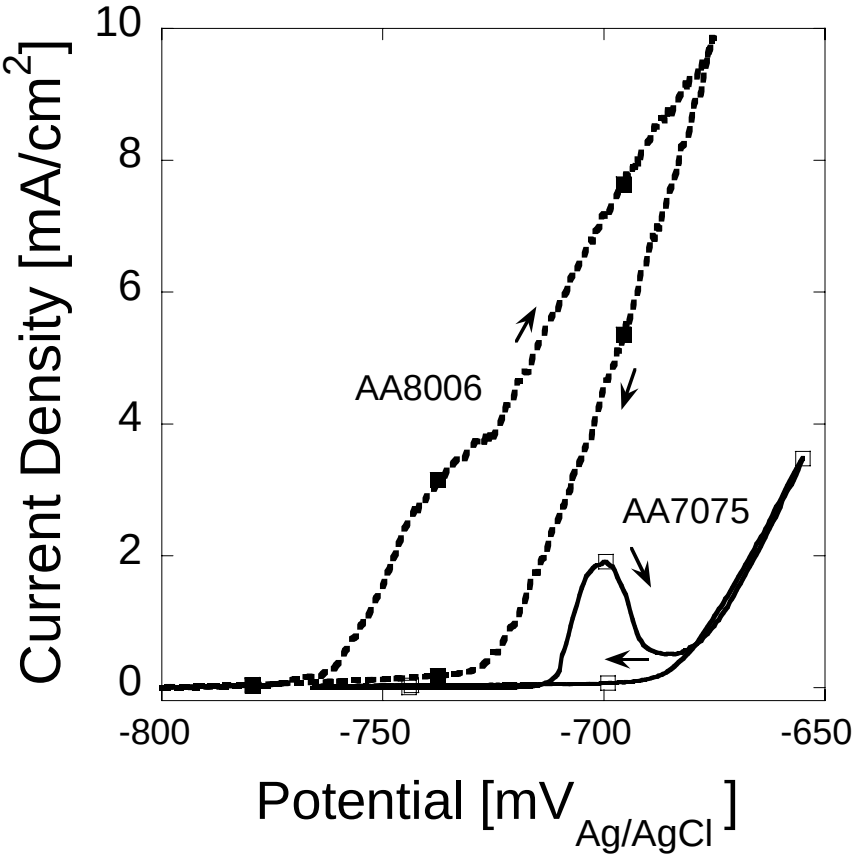

Figure 2. Polarization curves for abraded AA7075 and as received AA8006 in 0.5 M NaCl at a scan rate of 0.2 mV/s.

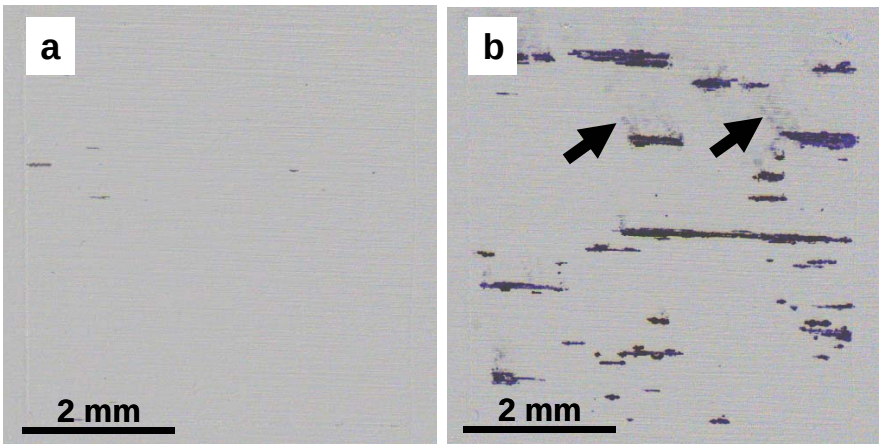

Figure 3. Images of as received AA8006 in 0.5 M NaCl

(a) A difference image obtained after subtracting and processing an image taken at 10 min from an image at 13 min.

(b) A difference image derived from an image at a current density of 0.5 mA/cm2 and a 3 min earlier image during the polarization scan shown in Figure 2.

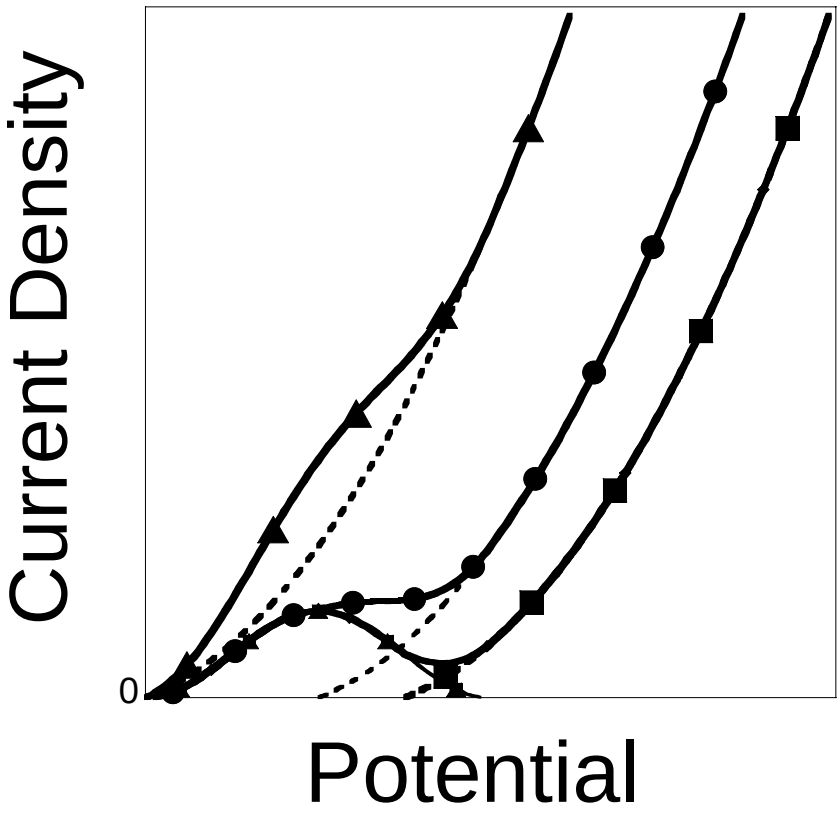

Figure 4. Schematic polarization curves showing the effects of changing the relative positions of the streaking and pitting susceptibility.